

# The impact of large-scale tunnel excavation on neighboring structures in dense urban areas: The characteristics of interaction

Lojain Suliman<sup>4</sup>, Xinrong Liu<sup>\*1,2,3,4</sup>, Changbao Jiang<sup>4</sup>, Xiaohan Zhou<sup>1,2,3</sup>,  
Yuxuan Chen<sup>1,2,3</sup> and Lei Fang<sup>1,2,3</sup>

<sup>1</sup>State key laboratory of coal mine disaster dynamics and control, China

<sup>2</sup>College of Civil Engineering, Chongqing University, Chongqing 400045, China

<sup>3</sup>State Key Laboratory of Coal Mine Disaster Dynamics and Control, Chongqing University, Chongqing 400044, China

<sup>4</sup>National Joint Engineering Research Center of Geohazards Prevention in the Reservoir Areas (Chongqing),  
Chongqing 400045, China

(Received August 27, 2024, Revised February 9, 2025, Accepted February 10, 2025)

**Abstract.** The traffic congestion in many cities in China especially during the peak hours has led to the building of new subways. The development of public transportation can reduce the use of private vehicles, thereby reducing road traffic congestion. In this paper, a case study in Chongqing City including a big tunnel section with a diameter of 26 m will be shown. In addition, two small tunnel sections laying orthogonal with the main tunnel (big section) will also be studied. Wind ventilation is located between the two small tunnels have also been excavated. To investigate the deformation characteristics of such dense excavation procedures 3D FEM model has been built. The numerical simulation resulting data with the site monitored determined points has been compared. However, the comparison shows good agreement. Moreover, according to some sections of the big tunnel which includes a dense urban area with the above structures, a raft building with different piles diameter as a foundation support has been considered. Based on the numerical simulation as an effective tool, huge data has been generated to investigate the extension of the spreading of the influenced zone due to the excavation of three types of tunnels: the first is the big tunnel section with a diameter of 26 m. The second is a tunnel section with 13 m. While, the final tunnel case is twin tunnels, each tunnel has a diameter of 13 m. These tunnel cases have been studied and the interaction between (different piles diameter + raft) systems and different tunnel diameters has also been investigated. The influenced area has been proposed according to each tunnel case. However, the results show that 'R' ratio which represents the pile settlement after the excavation divided by the pile settlement before the excavation has much more difference in comparison with the extension area of the disturbance.

**Keywords:** big tunnel section; dense urban areas; extension of the disturbance; influenced zone

## 1. Introduction

In general tunnels excavations have an impact on the surrounding environment. Especially when the resulting settlement affects the surrounding buildings and other existing structures. When tunneling goes through dense urban areas, the impact of soil settlements on existing buildings must be carefully estimated. Soil-structure interaction (SSI) systems are characteristically complex due to the effects of interfaces, soil non-linearity, and plasticity. An adjacent construction with a pile foundation in dense urban areas can contribute to possible damage to or an operational safety concern for existing tunnels.

The effect of excavating a tunnel on the surrounding structures has been investigated by previous scholars. (Franza *et al.* 2019) presented the outcomes from 24 geotechnical centrifuge tests that aim to investigate the salient mechanisms that govern piled building response to tunneling. The results show that the piles settlement due to tunneling depends on several factors such as the method of

installation for the piles which is also related to the factor of safety. (Ding *et al.* 2019) investigated two main issues such as the effect of excavation on structure stiffness and the most appropriate layout by using 3D finite element analysis, the results show that by decreasing the stiffness the deformation will increase. Moreover, as a general conclusion they found that the value, process and distribution of settlements differed under various rates of building stiffness. (Burd *et al.* 2000) described the interaction process between a tunnel, soil and a building by using 3D finite element analysis, the results show that the proposed approach is efficient, however, have the important advantage of being able to provide assessments that are based on a rational procedure to model the interaction effects between the building and the ground. (Farrell *et al.* 2014) used two tools which are the centrifuge test and the field measurements, the results revealed that the modification to settlement distortions is a function of both building and the soil stiffness, in addition to the geometric parameters. Moreover, a very important issue has been noticed related to the weight redistribution due to tunneling which significantly influences the response of the soil and buildings. (Hemeda 2022) used Plaxis software to simulate and assess the deformation and stability of different intricate underground structure. Furthermore, (Hemeda

\*Corresponding author, Ph.D.  
E-mail: liuxrong@126.com

2022) addressed the pressing issue of preserving subterranean heritage structures in Alexandria, Egypt, which are increasingly threatened by geo-environmental hazards such as rising sea levels and heavy rainfall due to climate change

(Franza *et al.* 2017) presented an elastic model for tunnel-pile-structure interaction with focusing on structural displacements resulting from tunnel excavation beneath piled frames or simple equivalent beams. However, the results show that the stiffness of buildings has a significant effect on the pile settlements and the resulting building deflections. (Giardina *et al.* 2015) used the finite element analysis to make validation with centrifuge test, the results show that numerical simulation results reflect the experiment behavior, which constitute good approach. (Losacco *et al.* 2014) developed a simplified structural model for the building that suits the finite element analysis. The results show that the simplified assumption is appropriate to the projects which includes tunnels. (Mirhabibi *et al.* 2013) used 3D and 2D finite element analysis in order to consider the effect of tunneling on the building deformation, the results show that that the three-dimensional modeling causes great differences in comparison with 2D modeling. (Tsinidis and technology 2018) considered the tunnel-soil-building interaction, the results show that when the left tunnel already crossed the building, during the passage of the shield tunneling through the building, uneven settlement was reduced between left-right tunnels. Even the previous mentioned studies related to the tunnel-building interaction system. However, few studies described the interaction between big tunnel section and two orthogonal parallel tunnels. To what related to pile-tunnel interaction many studies have been discussed the interaction process. (Gerheim Souza Dias 2017) clarified the regulations for the minimum distance between the tunnel and the pile by reviewing previous studies and concluded that there are two main mechanisms related to the tunnel effect on the pile: the first happens through degrading the pile base capacity. While, the second because of the relative displacement between the pile and the soil which induces a negative friction angle. (Marshall *et al.* 2015) used an analytical approach which is spherical cavity expansion to calculate the effect of excavating a tunnel on an existing pile. The results revealed the importance of taking the geometric parameters into consideration such as the pile and the tunnel depth. (Marshall and Engineering 2012) investigated the influence of excavating a tunnel on a structure such as a pile by reducing the confining pressure. (Franza *et al.* 2017) presented a study to investigate the pile-tunnel-structure interaction, the results illustrate how piled foundations increase the risk of structural damage compared to shallow foundations, whereas structural stiffness can reduce the building deformations. (Meguid *et al.* 2009) described the experimental investigation to examine the effect of existing piles installed in cohesive soil and extended to bedrock on the circumferential stresses developing in a newly constructed tunnel supported by a flexible lining system, he concluded that the piles in the close vicinity of the tunnel usually experience an increased stress level due to the stress redistribution around the excavated tunnel. (Zhang *et al.* 2018) used a simplified analytical method to improve the pile tunnel interaction prediction, the results are also compared with and without

considering the effects of tunnel-soil-pile interaction. However, the comparison shows that when the influences of lateral soil displacements are considered, the results are closer to the monitored in-situ data and the centrifuge test data. (Sohaei *et al.* 2020) made a review related to pile-tunnel interaction by physical modelling and found that the most common and effective measure that can be taken to control the ground displacement at the sources is jet and compensation grouting. (Mahmood *et al.* 2011) made a parametric study by FLAC to assess the extent of the settlement problem for tunnels execution near piles. The parametric study includes: changing the rock friction angle, changing the pile's vertical offset, changing the tensile strength of the rock and changing the cohesion. However, according to one of the studied parameters, the results show that when the vertical offset of the pile was changed, there were considerable effects on the settlement results. (Franza *et al.* 2021) investigated the response of the piles to tunneling by proposing a continuum-based model for soil pile interaction, the distinguished feature of this model is the capability to consider the nonlinear load transfer mechanism, the results show that the COMPILE model can reliably predict deep foundation response to vertical loads. Moreover, it should be mentioned that the validation has been done by making a comparison with field data.

In this paper, a big tunnel section has been excavated with two orthogonal small tunnel sections. In addition, a wind pavilion has been excavated vertically from the ground surface. The validation has been done with site measurements. Furthermore, in order to reveal the influence of such excavation in weak rock and to reveal the effect of the weak rock on the settlement characteristics, weak rock parameters have been selected according to the Chinese code. The novelty of this study lies in the excavation process in such a dense environment, which may cause tunnel interactions and lead to excessive settlement. Furthermore, determining the influence zone of tunnel excavation is very important for design purposes.

## 2. The project condition

In order to speed up Chongqing's urban construction and improve Chongqing's traffic environment. The west extension project of Rail Transit Line 4 has been built. The project includes a tunnel with a big section. The diameter of this tunnel reaches 26 m. In addition to, two main small tunnels section. The layout of the two small tunnels is orthogonal with the big tunnel section. The diameter of the first small tunnel is 10 m. While, the diameter of another one is 4.9 m. Moreover, in addition to the two main structures a wind pavilion has also been excavated in order to improve the ventilation process. The excavation of the big tunnel section is shown in Fig. 1.

### 2.1 The general geological conditions

The geotechnical engineering conditions of the west extension section of the proposed rail transit line 4 are moderately complex, the overall trend of the line is obliquely intersected with the geological structure line at a large angle.



Fig. 1 Big tunnel section in the real site

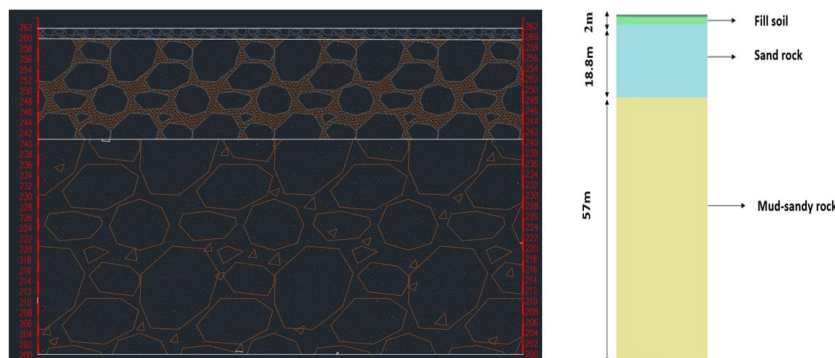


Fig. 2 The Geological profile

The thickness of the covering layer is 0.00-33.50 m, and the underlying bedrock is the Middle Jurassic sandstone. The sandstone and sandy mudstone of the Ximiao Formation are relatively complete rock mass; the hydrogeological conditions are simple, and the groundwater is mainly bedrock fissure water. The regional tectonic effect is slight, no faults have passed through, and no unfavorable geological phenomena such as dangerous rocks, collapses, and debris flows have been found. The current situation is generally stable. To sum up, the sites along the line are generally stable, suitable for the construction of the west extension of Metro Line 4, and the current line scheme is feasible. The Geological material properties are as shown in Fig. 2. The detailed geological conditions are as the following:

**Sandstone:** gray to purple gray, fine to medium-grained structure, thick layered structure; the main mineral components are quartz and feldspar, containing a small amount of mica and clay minerals, mostly calcareous cementation, local argillaceous cementation, hard rock, the integrity of the rock mass is good, and the basic quality grade of the rock mass is Grade III.

**Sandy mudstone:** mainly purple-red, the main mineral components are clay minerals, silty muddy structure, medium-thick layered structure, moderately weathered rock mass without cracks, rock mass is relatively complete, rock quality is relatively hard, and the rock mass is basically. The quality level is IV level.

**Fill soil:** artificial fill (including miscellaneous fill and plain fill), residual soil and strong weathered layer. Miscellaneous fill is mostly variegated, mainly composed of cohesive soil mixed with sandstone, mudstone broken stones, bricks, and concrete blocks, partially containing a small amount of construction and domestic waste, and the color is mainly dark brown after being soaked in domestic sewage. The plain fill is mostly purple-brown, mainly composed of cohesive soil inter-bedded with sandstone and mudstone crushed (block) stones, and partially contains a small amount of construction waste and domestic waste. The block stone content is 25-45%, the particle size is 60-1000 mm, and some parts can reach more than 1000 mm, the crushed stone content is 15-50%, and the proportion of block and crushed stone content has no connection with depth and location, which means is randomly distributed. Fig. 2 shows the soil profile for the area under study and the location of the big tunnel section.

## 2.2 The monitored points

Several monitored points in the site have been considered. These points have been distributed above the tunnel in the real site. For the big tunnel section 10 points have been distributed. However, due to some difficulties in the site the data for just 8 points have been got above the big tunnel section. However, the data from the rest of the points have not been collected. Furthermore, four points

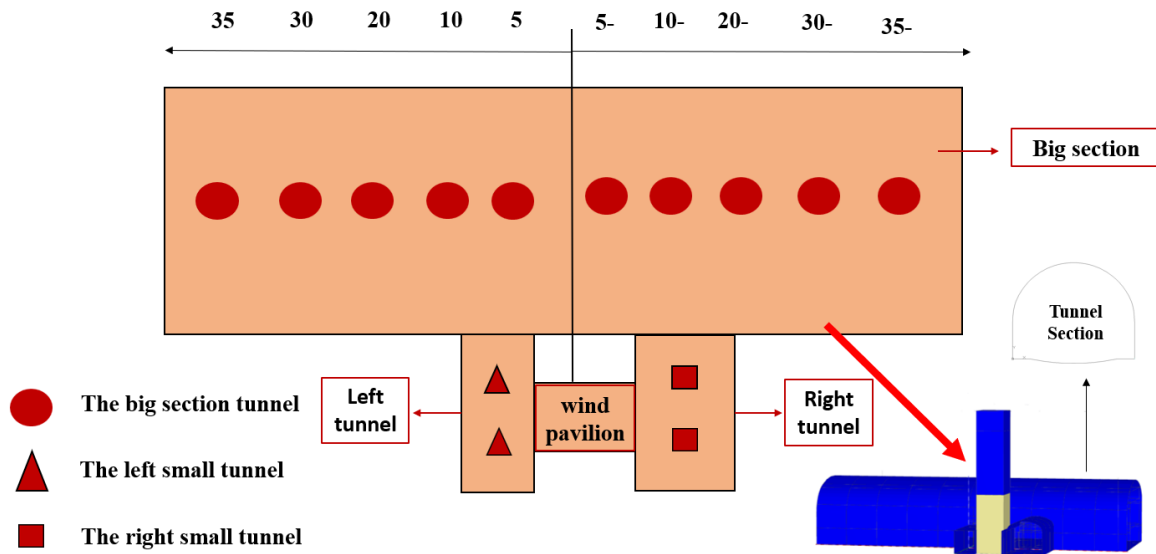


Fig. 3 Overall studied location

Table 1 Soil and rock parameters

Parameters	C (kPa)	$\Phi$ (degree)	E (kPa)	$\mu$	$\gamma$ (kN/m <sup>3</sup> )
Fill	5	25	20000	0.3	19.2
Sand rock	1500	36	2100000	0.17	24.8
Sand-mud rock	380	32	1020000	0.22	25.5

have been considered above the two tunnels. Two points above each tunnel. The settlement data have been collected and recorded with the time. Fig. 3 shows the layout of the monitored points.

### 3. Preliminary ground model

The field investigations indicate that there are three layers of soils and rocks. According to borehole data. Table 1 shows the parameters properties. Mohr-Coulomb has been used as a constitutive model. (Liu *et al.* 2022) used (M-C) model to make verification between the model test and the numerical simulation. The results Show that (M-C) is a good constitutive model in predicting the settlement behavior. For example, in the previous mentioned study M-C model has been used for both the fill soil and rock, in addition, a comparison between the HS model and M-C model for the fill soil has been done. However, the results show that M-C model is more appropriate in comparison with HS model. Key Components of the Mohr-Coulomb Model are: (1) Shear Strength Parameters such as the cohesion, the friction angle. The shear strength equation is expressed as follows

$$\tau = c + \sigma \tan(\phi) \quad (1)$$

The model assumes linear elastic behavior before yielding, defined by: Young's Modulus (E): Governs the material's stiffness. Poisson's Ratio ( $\nu$ ): Represents the ratio of lateral strain to axial strain during elastic deformation.

The material deforms plastically once the stress state reaches the failure envelope defined by the Mohr-Coulomb criterion. Additionally, there is consideration related to non-recoverable deformations after yielding. Mohr-Coulomb model operates using the concept of principal stresses, where the material's behavior is analyzed based on the maximum and minimum principal stresses.

Part of the mechanical tests results are shown in Fig. 4.

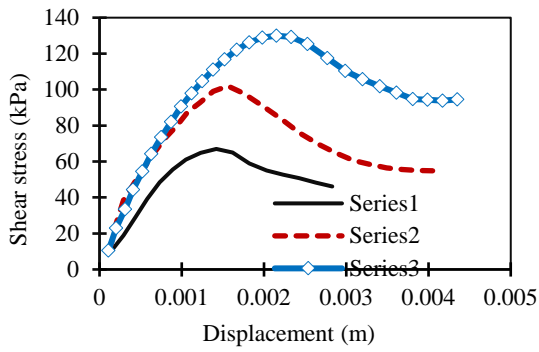
## 4. Results

The results will be shown in different parts according to the following: (1) validation between the site measurements and the finite element analysis for the big tunnel section and the two small tunnels. (2) Then a building has been considered after reducing the soil parameters. (3) A huge amount of data has been considered to investigate the extension of the influence zone and the amount of disturbance due to the excavation.

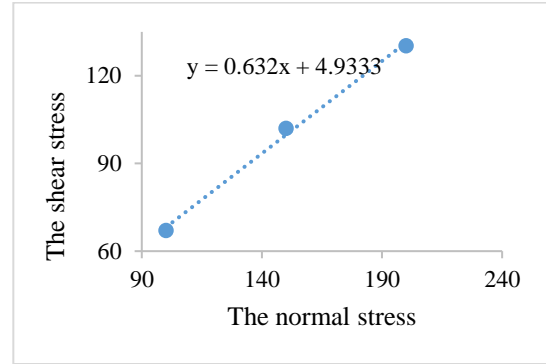
### 4.1 The validation between the site measurements and the finite element analysis

#### 4.1.1 The excavation of the big tunnel section

The following charts show the validation between the site measurements and the numerical simulation. Along the tunnel, several points have been selected as monitoring points. 8 main monitoring points have been selected. These points have been distributed along the tunnel in the middle long section (central section). The comparison between the site measurements and the numerical simulation shows good agreement. According to the site measurements, the maximum settlement has occurred in point (35) which is located at the edge of the big tunnel section. Moreover, the results show that the settlement dropped down when the excavation reached the monitored points. In general, the settlement range is between [19-26] mm. If the tunnel axis is divided into positive points and negative points, the



(a) The relation between shear stress and displacement

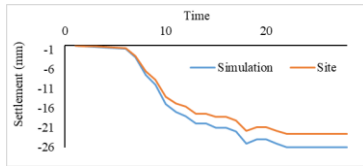


(b) The relation between the shear stress and normal stress

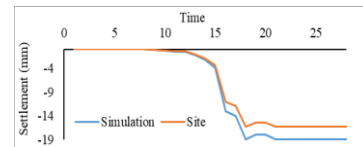


(c) The direct shear test device

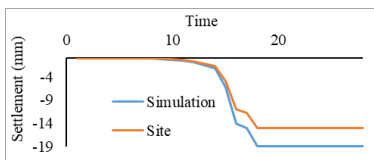
Fig. 4 The mechanical tests



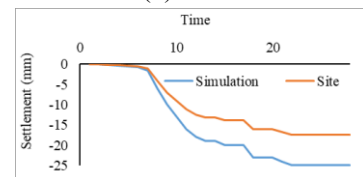
(a) 35 m



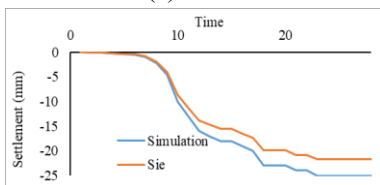
(b) -35 m



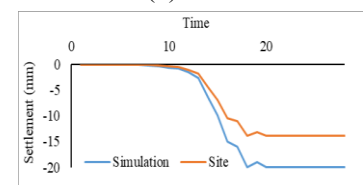
(c) -30 m



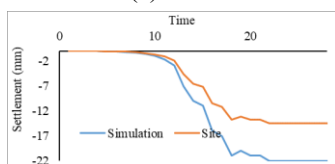
(d) 30 m



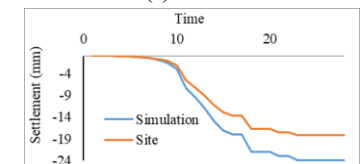
(e) 20 m



(f) -20 m



(g) -10 m



(h) 5 m

Fig. 5 The validation between the site measurements and the numerical simulation-points position

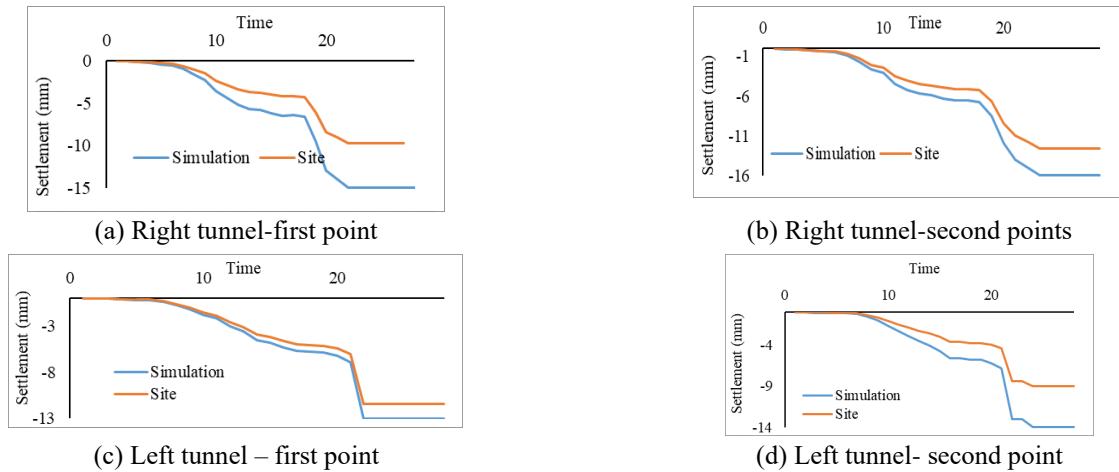


Fig. 6 The settlement in the two small tunnels

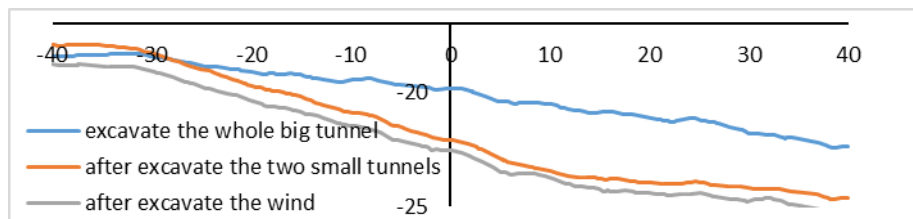


Fig. 7 The settlement variation for the studied tunnels

results show that the settlement values in the negative direction are smaller those that in the positive one. It is also clear that the settlement increases with time. When the excavation reaches the monitored section there will be a sharp increase in the settlement value. After making safety calculation, the results show that the factor of safety is 3.1. To calibrate the validation, first, the material properties have been ensured. Second the in-situ stress state and excavation sequence have been replicated. Then, the construction stages have been established according to the site case, after that, a comparison has been conducted between the numerical simulation and the site measurements, with focusing on key metrics such as maximum settlement, settlement trends over time, and differences between positive and negative points.

#### 4.1.2 The excavation of the two small tunnels

The following charts show validation between the site measurements and the numerical simulation. These points have been considered for the two small tunnels which located on the right and left. Two points above each section have been monitored. The right tunnel has been excavated first followed by excavating the left one. In the right tunnel, the second point has been settled more than the first point. The values of the maximum settlement according to the site data are (9.6 mm) and (12.5 mm). The difference between the site measurements and the numerical simulation is a bit more in the case of the first point of the right tunnel, in comparison with the second point. While, for the left tunnel, this difference is not big as much as the left one.

A long section has been considered in the middle of the big tunnel section. The results show that the settlement after

the excavation of each tunnel has been shown in the following figure. This figure shows that the settlement has increased after excavating the two small tunnels. The maximum settlement value was at the end of the tunnel section, which may be due to the influence of the accumulation of the excavation action. This value has been increased from 22.3 mm to 24.6 after the excavation of the two small tunnels. In addition, this value has been slightly increasing after the excavation of the ventilation part to a value of 25.1 mm. This slight increase may due to the excavation direction for the ventilation part which has been started from top to bottom. In addition, the small area of this excavated section leads to a small volume loss. Moreover, the excavation level has not been going down to the base of the long section level. Which means that the excavation level has not been reached the previous disturbed zone. From the sustainability aspect, it can be said that monitoring and analyzing the settlement after each excavation phase allows for more precise predictions and control of ground deformation, reducing risks to surrounding structures and ecosystems. The slight settlement increase during ventilation excavation demonstrates the importance of careful sequencing and controlled excavation methods to minimize ground disturbances and prevent widespread environmental impact. The findings suggest that excavation techniques, such as limiting the disturbed zone and sequential excavation, can reduce unnecessary material loss and energy usage, aligning with resource-efficient construction. Additionally, ensuring that settlements remain within acceptable limits enhances the durability and safety of the underground works, contributing to their long-term viability. By avoiding

Table 2 Rock parameters reduction

Parameters	C (kPa)	$\Phi$ (degree)	E (kPa)	$\mu$	$\gamma$ (kN/m <sup>3</sup> )
New rock	50	20	1.e6	0.39	20

Table 3 Rock parameters according to Chinese code

Level	Sub level	Gma (Kn/m3)	K (Mpa/m)	E (Gpa)	u	Phi (°)	C (Mpa)
Third level	1	24-25	850-1200	10.7-20	0.25-0.26	44-50	1.1-1.5
	2	23-24	500-850	6-10.7	0.26-0.3	39-44	0.7-1.1
Forth level	1	22-23	400-500	3.8-6	0.3-0.31	35-39	0.5-0.7
	2	20-22	200-400	1.3-3.8	0.31-0.35	27-35	0.2-0.5
Fifth level	1	18-20	150-200	1.3-2	0.35-0.39	22-27	0.12-0.2
	2	17-18	100-150	1-1.3	0.39-0.45	20-22	0.05-0.12

Table 4 Stand up time

class	1	2	3	4	5
Average stand-up time	20 yr for 15m span	1 Yr for 10m span	1 wk for 5m span	10h for 2.5 span	30 min for 1m span
Cohesion of rock mass (KPa)	>400	300-400	200-300	100-200	<100
Friction angle of rock mass (deg.)	>45	33-45	25-35	15-25	<15

excessive deformation or destabilization, the integrity of the underground system and adjacent structures is maintained, reducing future risks and costs.

## 5. Parametric study

### 5.1 Surrounding buildings consideration and Parameters re-consideration

The parameters which have been presented above are related to the real site condition and represent very strong rock. This means that under this type of parameters the settlement effect is very limited. Moreover, the results of the site parameters as has been presented in the previous sections and the settlement values which will be shown in the following parts have revealed this issue. However, in order to investigate the effect of excavating the big tunnel section in a weak rock when there is a superstructure above the big tunnel section, new parameters' reduction has been presented and this reduction will be according to another site parameters according to the Chinese code. The new parameters which have been used in the following section will be presented as the following. It should be mentioned that the two rock layers have been replaced by one rock layer. Table 2 shows the rock parameters. What is related to the excavation of such tunnels in dense urban areas, especially excavating such big tunnel sections will affect the surrounding building due to the big volume loss. During the excavation, many buildings have been encountered. Thus, in order to investigate the effect of excavating big tunnel sections in dense urban cases in more dangerous conditions. Rock parameters reduction has been considered.

This reduction has been done according to the Chinese code specification as shown in Table 3. However, this value will be taken according to the minimum parameter values. It should be mentioned that after reducing the rock parameters the stand-up time will also be less. Thus, in this type, the shotcrete has been directly erected after the excavation of each part in the different excavation methods. (Nguyen *et al.* 2015) made an analytical solution to investigate the stand-up time for rock mass. However, Table 4 shows the variation of stand-up time with varying rock properties. Furthermore, three types of buildings have been considered. The main difference in each building is the pile diameter. Three diameters have been considered according to the following: (d=0.2, d=0.3 d=0.4) m.

### 5.2 The base building parameters and Stage construction

Two main structures have been used to represent the building's foundation. The first is embedded beams. While, the second is the raft. The embedded beams have been represented by an embedded element. While, the raft has been represented by plate elements. The pile variation characteristics will be shown in the following table. As well as the plate characteristics. Table 5 summarizes the material parameters as has been used in Plaxis3D numerical simulation.

Several stage constructions have been implemented. The first is the initial stage which has been done according to 'K0'. While, in the second stage the plastic type was used. In this stage, the raft and the embedded beams have been applied. The next stages include the excavation procedures for four types of excavation which are the following: (1)

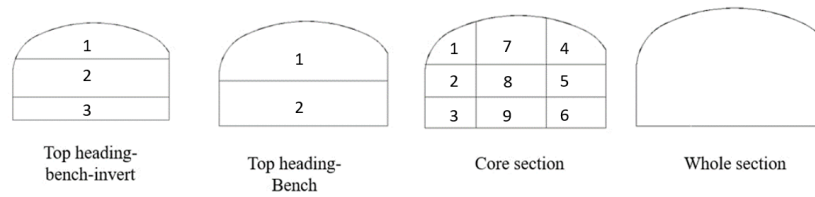


Fig. 8 The different excavation steps

Table 5 Building parameters and properties

Element	Diameter /plate thickness (m)	material	Length (m)
pile	0.2	concrete	5
pile	0.3	concrete	5
Pile	0.4	concrete	5
plate	0.3	concrete	-

core section excavation (2) Top heading-bench-invert (3) Top heading (4) Whole section. Fig. 8 shows the type of the excavation.

## 6. Developing the influence zone around the tunnel

### 6.1 The main concept of the influence zone

The concept for developing tunnel influence zones depends on a series of finite element models. In such cases, and after a series of sensitivity analysis, the results show that the tunnel diameter causes the maximum influence on the extent of the influence zone. This case study includes a big tunnel section. According to the tunnel diameter which is equal to 26m it is impossible to do the excavation in one step. Thus, four main methods have been used which are: ① Core section, ② top heading-bench, ③ top heading-bench-invert and ④ the whole section. Moreover, three main piles diameter have been considered to support the building which are the following: ('0.2, 0.3, and 0.4') m. Thus, the influenced zone will be affected by two main interaction actions: the first is the interaction between the piles. While, the second is the interaction between the piles and the big tunnel section. The legend will be developed according to the 'R' ratio. This ratio represents the pile displacement after the excavation/pile displacement before the excavation. Several previous studies have been used to investigate the extent of the excavation influenced zone. For example, (Jongpradist *et al.* 2013) developed a tunnel influence zone according to a series of finite element analysis which include data related to normalized pile settlement and maximum pile bending moment. The merit of the FEM model is the ability to generate a series of models, especially because the existing piles are nearly impossible to instrument to study their response, and physical model tests are expensive and time-consuming. This influential zone mainly depends on two main variables which are: The tunnel diameter and the pile diameter. Thus, in addition to vary the pile diameter, the tunnel diameter has

also been varied. Furthermore, to what related to the influence factor, different methods have been previously used to evaluate the influence of the excavation or the effectiveness of the used protective method. For example, (Bilotta *et al.* 2011) used an evaluation method to calculate the effectiveness of a vertical structural element for reducing the settlements induced by tunnelling. In the following sections, the results will be shown according to each case. The principles that have been implemented are the following:

- When the tunnel diameter is 26 m, the following areas have been considered according to the value of 'R' ratio, the maximum influenced area is between [200-250]. The medium influenced area is between [150-200]. The slightly influenced area is between [100-150]. While, the less influence area is [50-100].
- When the tunnel diameter is 13 m, the following areas have been considered. The maximum influenced zone has 'R' ratio as the following [25-30]. The medium influence between [20-25]. The less influenced one [15-20].
- When there are twin tunnel and each tunnel diameter is 13 m, the distribution of the influences zone is the same as the tunnel diameter equal to 26 m.
- The final classification of the extension of the influenced zone has been done according to the lower range of this extension in each excavation method and to the upper range of this extension.

### 6.2 Single tunnel ( $D=26$ m)

Three main cases have been considered for this pile diameter. This diameter variation has been considered under the effect of different excavation methods. These methods are the same as has been mentioned before. For the pile diameter of 0.2 m ( $d=0.2$  m), according to different excavation methods, the results show the following results:

- For 'Core excavation' method: the maximum value of 'R' ratio reached a maximum value of '167' in the pile tip location. This value is located in the influence range that was between (150 - 200) which represents the maximum influence range under this condition. However, in this case no ratio reached the value of '200'. The previously mentioned range has been extended to a distance equal to ( $3D/13$ ). While, the minimum influence area has a ratio located between (50-100). This influence zone has been extended to a distance equal to ( $5D/13$ ). In addition to the two previously mentioned areas, there is also an area with a medium influence. 'R' ratio in this area is in the range between [100-150].

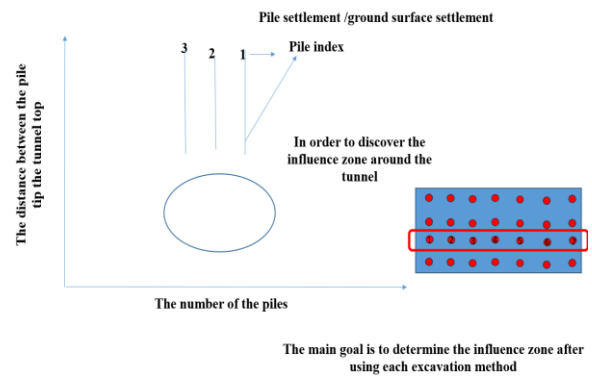
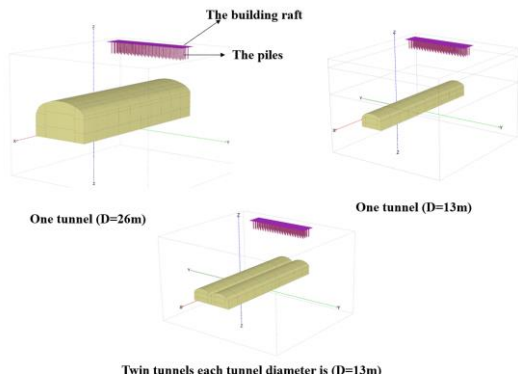


Fig. 9 The conceptual design

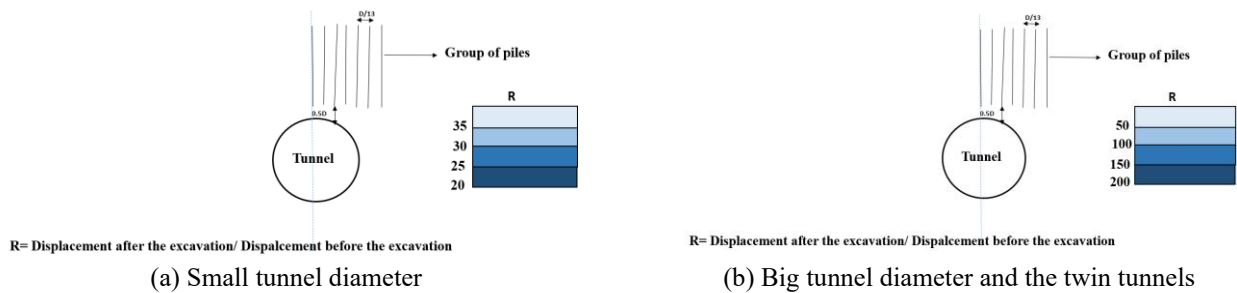


Fig. 10 The relation between 'R' ratio and the tunnel diameter.

- For the 'Top heading-Bench-invert' excavation method, 'R' ratio reached a value equal to more than 250. This effect has been extended to a distance equal to  $(3D/13)$ . And this is the biggest influence rang in the whole excavation methods for this pile diameter. Moreover, 'R' ratio was between '200 -250' in a distance equal to  $(2D/13)$ . In the 'invert excavation method', the less effect zone was in the area of  $(2D/13)$  which is related to a ratio located in the range (50-100). It can be considered that under this condition, the less influenced area is relatively small.
- In the 'Top-heading Bench' excavation method: the maximum value of 'R' ratio has been reached to a value of 250. This maximum influenced area which is located directly above the tunnel extended at a distance equal to  $(4D/13)$  forms the most influence zone. Furthermore, 'R' ratio for the next influence zone is between (150 -200) and extends to a distance equal to  $(2D/13)$ . The following influenced area is also extended to a distance equal to  $(2D/13)$ . However, the less influence zone is located at a distance equal to  $(8D/13)$  from the tunnel center line. Moreover, the maximum influence zone is relatively big with an 'R' ratio located between [50-100].
- In the 'whole section excavation method', the whole part of the piles have been assumed to 'R' ratio in a range located between (100 -150). While, only one pile has been assumed to have a ratio located between (50 -100). The less affected pile is the pile which located far from the tunnel's vertical centerline. Furthermore, it should be mentioned that in order to complete the excavation procedures in this area and avoid failure,

grout has been injected in the area which located under the building and above the big tunnel section. This means that this minimum range of 'R' is due to the grout injection.

When the piles diameter equal to 0.3 ( $d=0.3$  m), the results illustrate that 'R' ratio as the following:

- For 'Core excavation method' 'R' ratio in the position of the pile tip has been reached to a value exceeding '134'. In this case, the pile which located in the centerline of the tunnel has the maximum effect. While, the 'R' ratio for the next group of piles is located between (100-150) and this effect extended to a range equal to  $(4D/13)$ . Finally, 'R' ratio in the less influence zone which has values between [50-100] extended to a distance of  $(7D/13)$ .
- In the 'Top heading-bench-invert' excavation method the maximum influence area has been extended to a value of  $(4D/13)$ , 'R' ratio in this area is located [200-250]. The next influence zone extends to a distance of  $(3D/13)$  and is located between [100 -150]. However, under this excavation method condition the less effective zone is located over a distance of  $(2D/13)$ , and 'R' ratio in this area is located between [50-100].
- For the 'Top heading-bench' excavation method, the maximum influenced area is located over a distance of  $(3D/13)$ . 'R' ratio in this area is in the range of [200-250]. The second influenced zone extended to a value of  $(2D/13)$ . Moreover, 'R' ratio has a value of [150-200]. The less influenced area is located over a distance of  $(4D/13)$ , and 'R' ratio in this area is in the range [50-100].
- In the 'whole excavation' method, the most influenced area extended over a distance of  $(10D/13)$

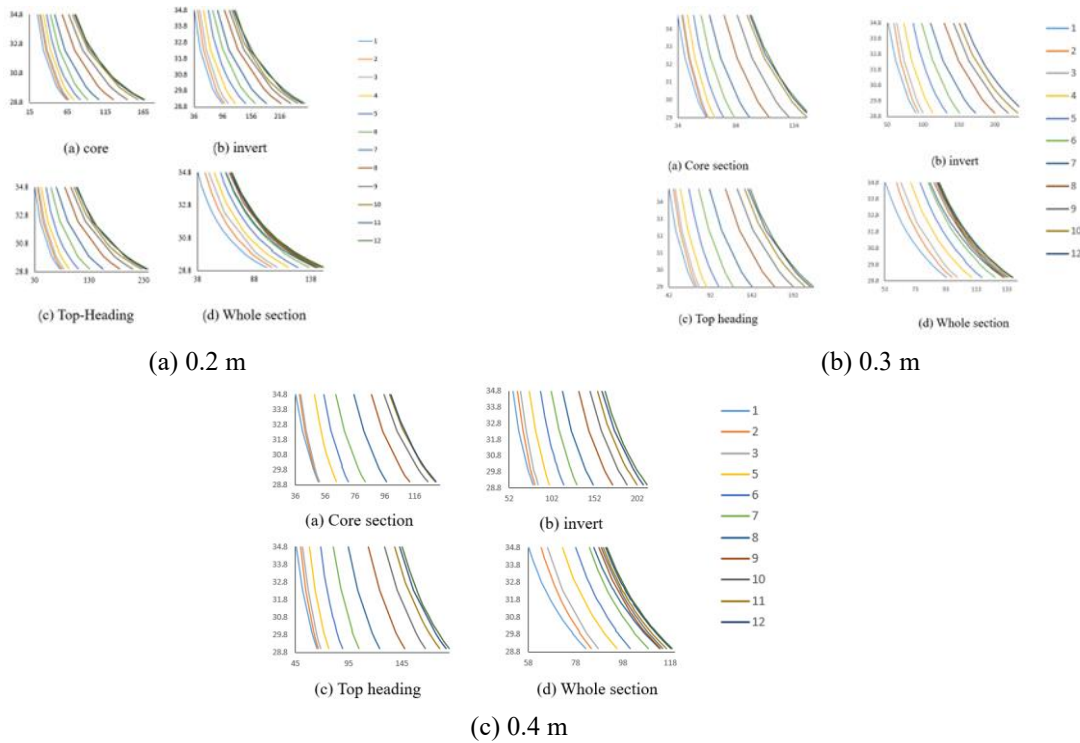


Fig. 11 The pile diameter is 0.4 m

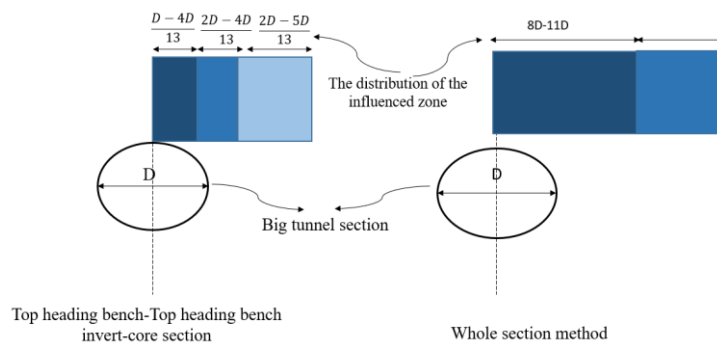


Fig. 12 The influenced zone according to the previous study

and located in the range of [100-150]. While, the next influenced part is extended over a distance of  $(2D/13)$  and located in the range of [50-100].

When the pile diameter equal to 0.4 ( $d=0.4m$ ). The results show that:

- For the ‘Core section’ excavation method, the most influenced zone is over a distance of  $(4D/13)$  with ‘R’ ratio located in the range of [100-150]. While, when the range of ‘R’ ratio is between [50 -100] the influenced zone is over a distance of  $(8D/13)$ .
- In the ‘Top heading-bench-invert’ excavation method, the maximum influenced area is over a distance of  $‘3D/13’$  and ‘R’ ratio range is between [200-250]. The next influenced zone is extended over a distance of  $(3D/13)$  with a range between [150-200]. The next zone extended over a distance of  $‘2D’$  with ‘R’ ratio between [100-150]. However, the less influenced zone is extended over a range of  $(4D/13)$ .

- In the case of ‘Top heading’ excavation method, there are three main excavation areas distributed as the following:  $(‘4D/13, 3D/13, 5D/13’)$ , ‘R’ ratio is as the following:  $‘[150-200], [100-150],[50-100]’$  for the three previous mentioned extensions respectively. The less influenced area spreads over a distance of  $(5D/13)$ .

- For the last excavation method ‘whole section’, there are two main parts extended as the following  $(‘8D/13, 4D/13’)$  for the range  $([100-150], [50-100])$  respectively.

For the ‘core section’ excavation method, it was noticed that when the pile diameter is 0.2 m the maximum influence zone will extend over a distance of  $(3D/13)$ . With increasing the pile diameter, the maximum influence zone will spread over a distance of  $(D/13)$ . Which means that with increasing the pile diameter the extension of the influence zone will be diminished. Moreover, when the pile diameter is increased to 0.4 m there will be two influenced zones. However, it is

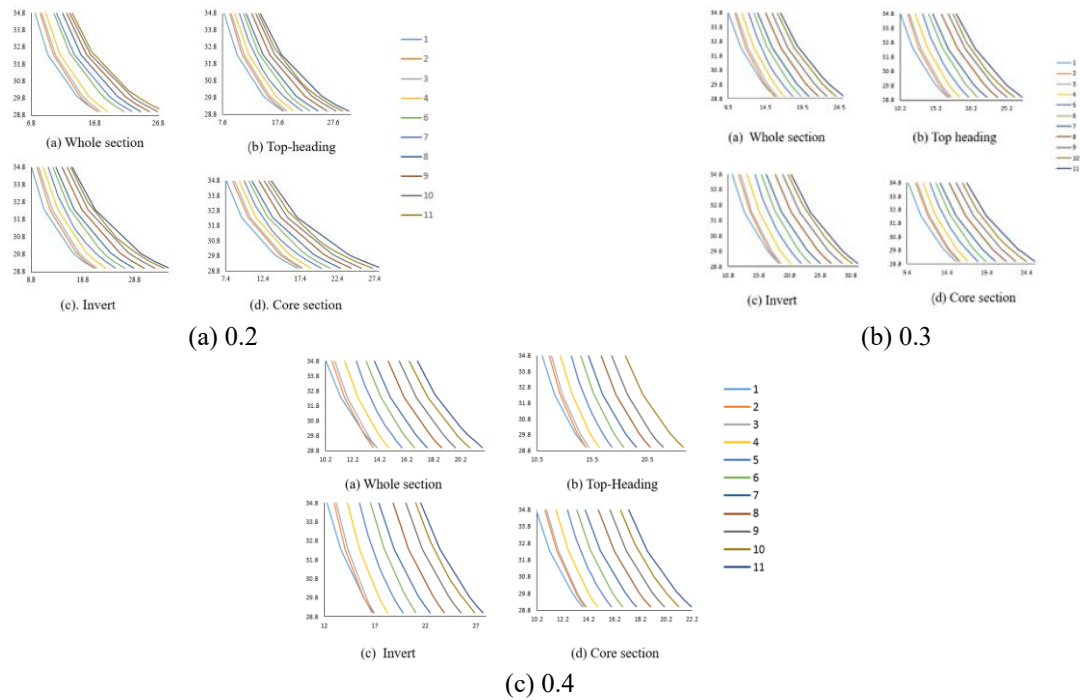


Fig. 13 The tunnel diameter 13 m

obvious that ‘R’ ratio has fewer values when the pile diameter has been increased. For example, when the pile diameter is 0.2 and 0.3 the range of the maximum influence zone is between [150-200]. While, when the pile diameter is 0.4, this zone will be between [100-150]. In the ‘invert’ excavation method, when the pile diameter is 0.2 m, ‘R’ ratio for the maximum influenced zone will be more than 250. While, for the two remaining piles ‘diameter the maximum influenced area is between [200-250]. It is also clear that with increasing the pile diameter is extension of the maximum influenced area will be less. In the ‘Top heading- excavation’ method the less influenced area extends to a zone equal to  $(5D/13)$  when the pile diameter is 0.4. And equal to  $(4D/13)$  when the pile diameter is equal to 0.3. Finally, this area diminishes to an area of  $(D/13)$  when the pile diameter is 0.2. This lead to consider that increasing the pile diameter can also leads to increase the minimum effect. In the ‘whole section’ excavation method, two main parts of the influenced zone have been noticed. However, as has been mentioned before with increasing the pile diameter the extension of the maximum influence zone will be decreased and the extension of the minimum influence zone will be increased. To sum up, the influence zone for this case can be considered as two main types. The first model of the influenced zone is for the three methods of excavation which are: ‘Top heading, Top Heading-Bench-Invert, and Core section’. While, the second one is for the ‘Whole section excavation method’. In the first model of influence, there are three main zones that will be extended as the following: Maximum influence  $(D/13$  to  $4D/13)$ . Medium influence  $(2D/13$  to  $4D/13)$ . While, the less influenced zone will be spread over a distance of  $(2D/13$  to  $4D/13)$ . The less influence zone spread over a distance of  $(2D/13$  to  $5D/13)$ . For The ‘Whole section excavation

method’ the maximum influenced zone is over a distance of  $(8D/13-11D/13)$ .

### 6.3 Single tunnel (D=13 m)

Three main cases have been considered for the pile diameter. This diameter variation has been considered under the effect of different excavation methods. These methods are the same as has been mentioned before. The proposed pile diameters are as the following: ‘d=0.2, d=0.3, d=0.4’. When the Pile diameter is 0.2 m, the results show the following:

- ‘Core section’ excavation method the range of the maximum influenced area is located between [25-30] and extended over a distance of  $(3D/6.5)$ . The less influenced area is spread over a distance of  $(4D/6.5)$  in a range between [15-20].
- ‘Top Heading-Bench-invert’ excavation method, the results show that the ‘R’ ratio range reaches a maximum value in comparison with the previous case. For example, in this case of the ‘core-section’ excavation method the maximum influenced area has the range of [25-30]. While, in this case the maximum value was between the range of [30-35]. Furthermore, the extension of the maximum and minimum influenced area is the same.
- ‘Top heading- Bench’ excavation method the maximum influenced area extended over a distance of  $(4D/6.5)$  in the range of [25-30]. This range is the same in the case of ‘Whole excavation’ method while the extension is less and reaches a value of  $(3D/6.5)$ .

When the piles diameter is equal to ‘0.3 m’ and ‘0.4 m’ respectively, the following results have been shown. First when the ‘core-section’ excavation method was used: two

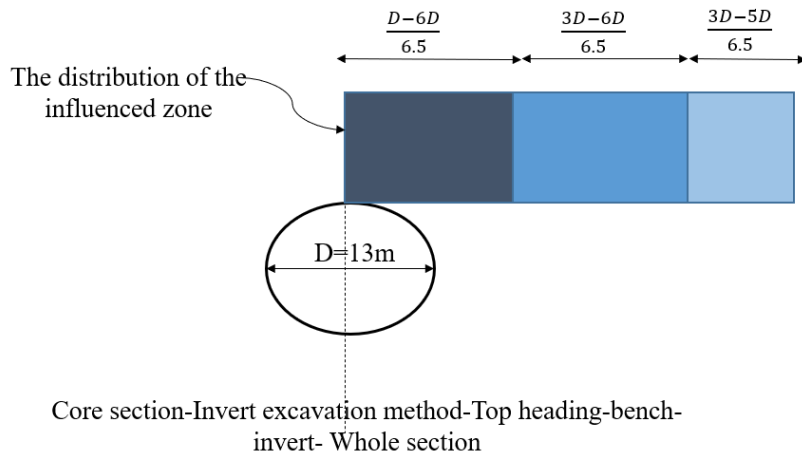


Fig. 14 The influenced zone according to the previous investigation

main areas appeared when the tunnel diameter was '0.3 m' the first one extended to a distance of  $(5D/6.5)$  and the second one extended to a distance of  $(6D/6.5)$  for the range of [20-25] and [15-20] respectively. Whereas when the pile diameter is '0.4 m' three main areas appeared according to the following classification:  $[(3D/6.5)$ ,  $(4D/6.5)$  and  $(4D/6.5)$ . With 'R' ratio range as the following: ([20-25], [15-20] and [10-15]). For the 'Top heading- Bench- Invert' the results show that when the pile diameter is '0.3 m' the maximum influenced area has a range of [30-35]. Whereas when the pile diameter is 0.4, this range has been decreased to a value of [25-30]. Moreover, the less influenced excavation area is more when the pile diameter increased to a value of '0.4 m'. In the 'Top heading- Bench' excavation method the results show that the extension of the maximum influenced zone when the pile diameter is '0.3 m' is bigger than that when the pile diameter is '0.4 m'.

The previous results show that in the whole excavation methods the 'invert excavation method' shows the maximum 'R' ratio value. In addition, according to the previously shown data, the results show that in the 'core excavation' method for the pile diameter of 0.2 and 0.4 ( $d=0.2$  and  $d=0.4$  m), there are three main influenced zones. The extent of each zone is as the following:  $[3D/6.5, 4D/6.5, 4D/6.5]$ . While, when the pile diameter is 0.3 m, there are two main areas that extend as the following:  $5D/6.5$  and  $6D/6.5$ . For the 'invert excavation method' the results show that for each diameter there is a different extent for the influenced area. For example, when the pile diameter is equal to 0.2m, there are three main distributed areas as the following:  $[4D/6.5, 3D/6.5$  and  $4D/6.5]$ . When the pile diameter is equal to 0.3, the extended influenced zones are as the following:  $2D/6.5, 3D/6.5, 3D/6.5$  and  $3D/6.5$ . Furthermore, when the pile diameter is equal to 0.4 m, the results show that the influenced areas are distributed as the following:  $3D/6.5, 3D/6.5$  and  $5D/6.5$ . For the 'Top-heading' excavation method, the results show that when the pile diameter is equal to 0.2 and 0.4 ( $d=0.2$  m and  $d=0.4$  m), the main disturbed areas extended as the following:  $[4D/6.5, 4D/6.5/3D/6.5]$ . When the pile diameter is 0.3 there are two main influenced areas as the following:  $6D/6.5$  and  $5D/6.5$ .

In general, the extended influenced area can be classified as the following: for the 'core section' excavation method, the most influenced zone extends in the range of  $[D/6.5-5D/6.5]$ , While, the medium influence  $[4D/6.5-6D/6.5]$ . Finally, the less influence is over a distance of  $[4D/6.5]$ . For the 'invert excavation' method, the results show that there are three main influenced areas: the most influenced zone is located between the range of  $[2D/6.5-4D/6.5]$ . The medium range is distributed over a distance of  $3D/6.5$ . At the same time, the less influenced area is extended between  $[3D/6.5-5D/6.5]$ . For the 'Top- heading' excavated method, the results show that the influenced area will be as the following: the most influenced area  $[4D/6.5-6D/6.5]$ . The medium influence is extended over the range of:  $[4D/6.5-5D/6.5]$ . While, the less effective area is over a distance of  $[3D/6.5-5D/6.5]$ . For the 'whole section' excavated method, the results show the following classification: the most influential area is located between  $[2D/6.5-5D/6.5]$ . The medium influence area is over a distance of  $[4D/6.5-6D/6.5]$ . While, the less influenced area is distributed over a distance of  $[4D/6.5]$ . After analyzing the whole previously mentioned data and as a conclusion it can be said that the influenced area is distributed as the following: the most influenced area  $[D/6.5-6D/6.5]$ . The medium influence  $[3D/6.5-6D/6.5]$ . While, the less influenced area is distributed over a distance  $[3D/6.4-5D/6.5]$ .

#### 6.4 Twin tunnels each tunnel diameter of 13 m

Twin tunnel sections are equivalent to one tunnel diameter of 26m. Each tunnel with a diameter of 13m and equal to the big tunnel section with a diameter of 26m has been considered. Three piles diameters have also been considered in this study. These diameters have been considered the same as in the previous cases. According to the selected pile diameter, the results are as the following:

- When the pile diameter is 0.2: For the whole methods of excavation, 'R' ratio in the piles tip is between '50-224'. In more details, In the case of 'core section' method of excavation 'R' ratio ranges between

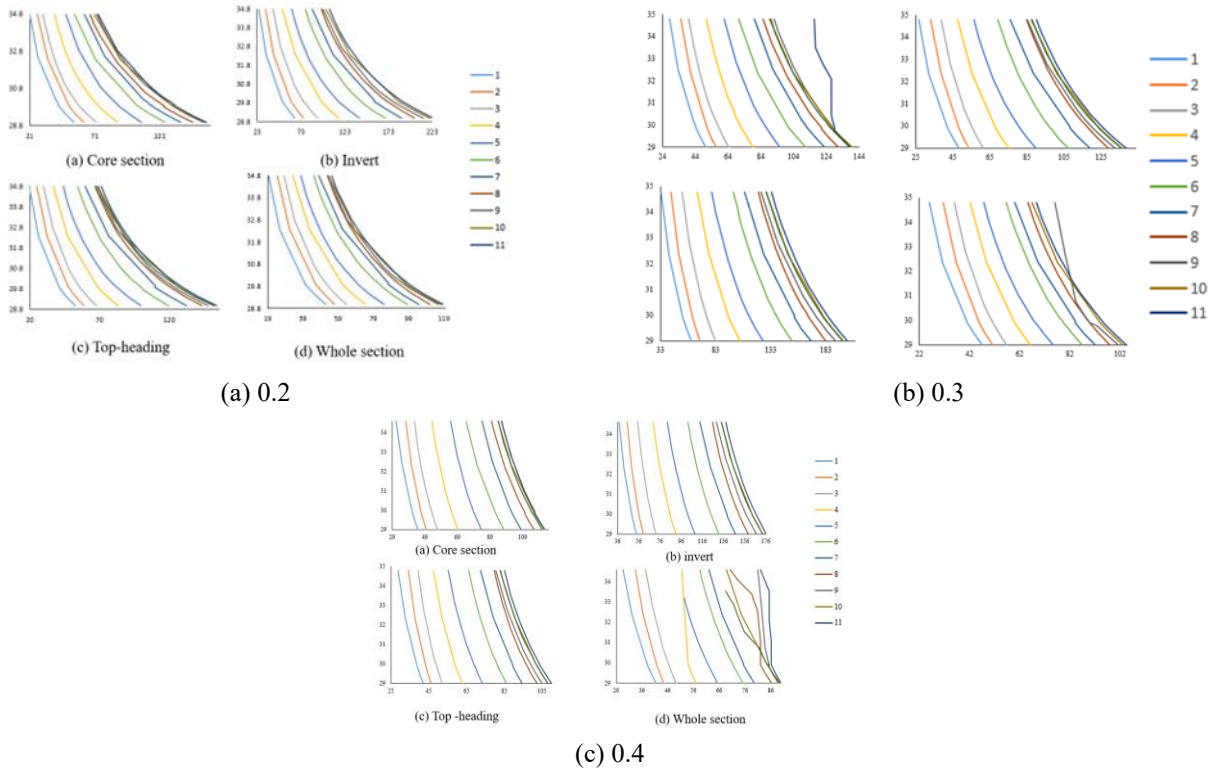


Fig. 15 The pile diameter is 0.3m

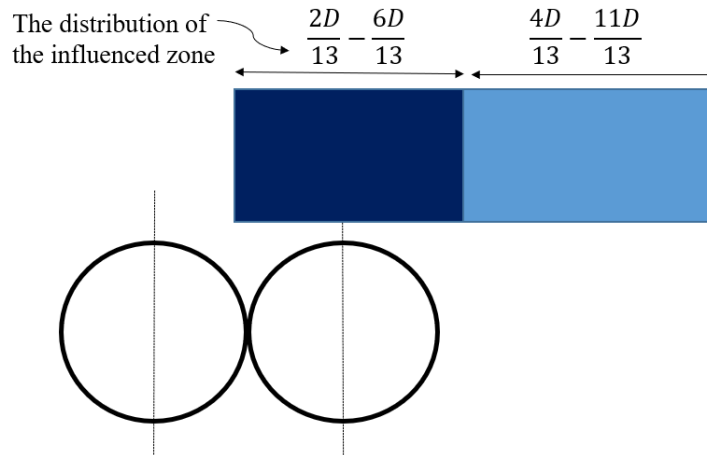


Fig. 16 The influenced excavation area

[ 51-118]. In the ‘Invert excavation’ method ‘R’ ratio is between [66-224]. In the ‘Top- heading’ excavation method it ranges between [52-152]. Finally, in the ‘whole excavation’ method this range is between [51-118].

- When the pile diameter is 0.3m. ‘R’ ratio in general ranges between [46-198]. In the ‘core section’ excavation method, ‘R’ value is between [50-138]. In the ‘whole section’ excavation method ‘R’ ranges [48-136]. In the ‘Top heading- bench-invert’ excavation method ‘R’ is between [60-198]. While, in the ‘Top heading- bench excavation’ method ‘R’ is between [48-136].

- When the pile diameter is 0.4m, the results are as the following: In the ‘Core section’ excavation method, ‘R’ is between [44-121]. In the ‘whole section’ excavation method R is between [41-88]. In the ‘Top heading-bench’ ‘R’ is between ‘42-108’. Finally, in the ‘Invert’ excavation method ‘R’ ranges from [53 to 172]. It is obvious from the whole method of excavation that the ‘Top heading-bench-invert’ causes the maximum influence. This influence has been also noticed in the pile’s diameter which is equal to 0.2m.

To what related to the extent of the influence zone, when the pile diameter is 0.2 m, under the ‘core section’ method excavation, the maximum influenced zone has been extended to a distance of (3D/13). Under the ‘Top heading-

bench-invert' excavation method, the maximum influenced zone reaches to a distance of  $(4D/13)$ . In the 'Top-heading – bench' the maximum influenced zone reached to a distance of  $(2D/13)$ . While, in the 'Whole excavation' method this zone is distributed over a distance of  $(5D/13)$ . When the pile diameter is equal to 0.3 m under the 'core section excavation method' the most influenced excavation area is distributed over a distance of  $(6D/13)$ . In the 'Top heading-bench' excavation method the maximum influenced zone is distributed over a distance of  $(6D/13)$ . In the 'Top heading-heading-invert' excavation method the most influenced area is distributed over a distance of  $(D/13)$ . In the 'whole section' excavation method the most influenced area is distributed over a distance of  $(3D/13)$ . When the pile diameter is equal to 0.4m. The 'core section' excavation method distributed over a distance equal to  $(5D/13)$ . In the 'invert excavation' method, the most influenced zone is distributed over a distance of  $(4D/13)$ . Finally, in the 'whole section' excavation method and 'Top heading- bench' extended over a distance of  $(4D/13)$ . In the 'whole section' excavation method, the influenced area is distributed over a distance of  $(11D/13)$ .

According to the previous data, the influence zone in this situation will be according to the following: The most influence zone is distributed over a distance of  $[2D/13-6D/13]$ . While, the next influence zone is distributed over a distance of  $(4D/13-11D/13)$ .

## 7. General discussion

By comparing the influence zone in the two cases which are different tunnel diameters  $D=26$  m and  $D=13$  m. The results show that the extension of the most influential area in the  $D=26$  m is  $[D/13-4D/13]$  in the whole excavation methods except the 'whole excavation section' method. While this area when the tunnel diameter is 13 m is distributed over a distance of  $[D/6.5-6D/6.5]$ . For the next influence area when the tunnel diameter is 26 m is distributed over a range  $[2D/13-4D/13]$ . While, when the tunnel diameter is 13 m, the medium influenced zone is extended over a distance of  $[3D/6.5-6D/6.5]$ . It is obvious that when the tunnel diameter is 26 m, the extension of the maximum disturbance area will be less in comparison with the tunnel diameter of 13 m. While, for the medium and the less influence area in the case of the tunnel diameter equal to 26 m, the extension of the disturbed area will be longer in comparison with the tunnel case of  $D=13$  m. Thus, even 'R' ratio in the case of ( $D=26$  m) is bigger in comparison with the case of ( $R=13$ ). This means that even with the high difference in the value of 'R' ratio but the extended of the distribution has slightly different values. In other words, the value of 'R' ratio has big difference, but at the same time the length of disturbance has not much difference.

By making a comparison between the influence of the excavation of the big tunnel section ( $D=26$  m) and the twin tunnels with the equivalent diameter, the results show that 'R' ratio does not have that much difference in the two cases. Regarding what is related to the disturbance of the extended area, the results show that in the case of the twin tunnel, the disturbance area is spread over a longer distance, in comparison with the big tunnel section. For example, the

maximum influence area in the case of twin tunnels spread over a distance of  $(2D/13$  to  $6D/13)$ . Whereas in the case of a big tunnel section this area will be spread over a distance of  $(D/13$  to  $4D/13)$ . In a conclusion, even 'R' ratio has a big difference when making a comparison between the ( $D=13$ ) and the two cases ( $D=26$  m) and (Twin tunnel each one has a diameter of 13 m). However, the length of the disturbance area has not much difference.

## 8. Conclusions

This study has explored various excavation procedures in dense urban environments, focusing on the impacts of tunnel excavation on surrounding structures and soil settlement. A case study involving a large tunnel section with two tunnels, along with ventilation considerations, was presented to understand the complexities of such projects. Settlement monitoring at the site, combined with a 3D FEM model and field measurements, provided valuable insights into the effects of excavation activities. The interaction between tunnel excavation and pile movement was also investigated through a series of numerical data, highlighting the excavation influence zone above the tunnel. Additionally, the 'R' ratio was used to assess the influence of excavation on surrounding areas. The findings underscore the importance of integrated monitoring, advanced modeling techniques, and careful consideration of excavation methods in urban tunnel construction. By linking numerical simulations with real-world data, this research contributes to a deeper understanding of how excavation processes affect surrounding infrastructure and offers practical guidelines for future projects in similar conditions. Ultimately, further studies should focus on refining excavation methods and exploring mitigation measures for minimizing settlement in densely built urban environments. As urban construction continues to expand, adopting such comprehensive approaches will be critical for ensuring the safety and stability of underground structures and minimizing the impact on surface-level infrastructure. The results can be concluded as follows:

- The site measurements show good agreement with the numerical simulation, which leads that the linear elastic perfectly plastic Mohr-Columb (M-C) model seems as good constitutive model in predicting the values in the site and the difference does not exceed 20%. Furthermore, after making a comparison of the settlement of the long tunnel section after the excavation of the three proposed tunnels, the results show that the settlement of the big tunnel section is the biggest reaches a value of almost 20 mm and after the excavation of the two small tunnels, there is no much difference in the settlement value, this is may related to the concept of the volume loss. For example, the maximum volume loss has happened due to the excavation of the big tunnel section. However, after that and because the two other tunnels have small diameters. Thus, no much volume loss.
- In order to discover the influence of the excavation influenced zone due to excavate the big tunnel section, a reduction of the rock parameters has been done

which leads to show the effect of the settlement on the above building. Basically, this influenced zone is due to three main factors which are the pile diameter ( $d$ ), and the tunnel diameter ( $D$ ). In addition to the excavation methods. However, in general the results show that the ‘core section’ excavation method shows the less settlement value. Furthermore, when the ‘whole section’ excavation method has been used to excavate the big tunnel section, the results show the grout injection needs to be used, especially because without this kind of support injection the excavation will be assume to failure.

- After making variation for the pile diameter, the results show that the tunnel diameter is still the decisive factor in the influence range of the effect of excavation. Which means that the volume loss is still the most influence factors on the pile movement. However, with increasing the pile diameter, the influence of the movement will also be less. Furthermore, according to the variation of the tunnel diameter the results show that, ‘R’ ratio has much more difference in comparison with the extension of the disturbance area. Thus, to what related to this point, it can be conclude that the tunnel diameter has more influence on the movement in comparison with the extension of the disturbance zone.
- The extension of the maximum disturbed area for the three previous cases is as the following: when the tunnel diameter is 26 m the extension of the influenced zone is over a distance of  $(4-4D/13)$  in the (top heading, top heading-invert, core section) excavating methos. While, this area distributed over a distance of  $(8D-11d/13)$  in the ‘whole section’ excavation method. When the tunnel diameter equal to 13m, the maximum influenced zone distributed over a distance of  $(D-6D/6.5)$  in the whole excavation methods. When the twin tunnels have been investigated, the disturbed area is over a distance of  $(2D/13)$  to  $(6D/13)$ . Moreover, it has been noticed that the ‘Top Heading-Bench-Invert’ excavation method cause the maximum settlement for the piles.
- Based on the relation between the pile diameter and the disturbed area, the results show that with increasing the pile diameter the extension of the influenced area will be less. In addition, it is obvious that ‘R’ ratio has less values when the pile diameter has been increased. Finally, with increasing the pile diameter, the extension of the less influenced zone will be extended.
- For future research, it is recommended to study this case under the seismic performance. Furthermore, it is very important to support these statistics with more experimental studies.

## Acknowledgements

This work was supported by the National Key R&D Program of China (Grant No. 581 2018YFC1504802), National Natural Science Foundation of China (Grant No.41972266).

## References

- Bilotta, E. and Russo, G. (2011), “Use of a line of piles to prevent damages induced by tunnel excavation”, *J. Geotech. Geoenviron. Eng.*, **137**(3), 254-262. [https://doi.org/10.1061/\(ASCE\)GT.1943-5606.0000426](https://doi.org/10.1061/(ASCE)GT.1943-5606.0000426).
- Burd, H.J., Houlsby, G.T., Augarde, C.E. and Liu, G. (2000), “Modelling tunnelling-induced settlement of masonry buildings”, *Proceedings of the Institution of Civil Engineers: Geotechnical Engineering*, **143**(1), 17-29. <https://doi.org/10.1680/geng.2000.143.1.17>.
- Ding, Z., Ji, X., Li, X. and Wen, J. (2019), “Numerical investigation of 3D deformations of existing buildings induced by tunnelling”, *Geotech. Geol. Eng.*, **37**, 2611-2623. <https://doi.org/10.1007/s10706-018-00781-1>.
- Farrell, R., Mair, R., Sciotti, A. and Pigorini, A. (2014), “Building response to tunnelling”, *Soils Found.*, **54**(3), 269-279. <https://doi.org/10.1016/j.sandf.2014.04.003>.
- Franza, A. and Marshall, A.M. (2019), “Centrifuge and real-time hybrid testing of tunneling beneath piles and piled buildings”, *J. Geotech. Geoenviron. Eng.*, **145**(3), 04018110. [https://doi.org/10.1061/\(ASCE\)GT.1943-5606.0002003](https://doi.org/10.1061/(ASCE)GT.1943-5606.0002003).
- Franza, A., Marshall, A.M., Haji, T., Abdelatif, A.O., Carbonari, S. and Morici, M. (2017), “A simplified elastic analysis of tunnel-piled structure interaction”, *Tunn. Undergr. Sp. Tech.*, **61**, 104-121. <https://doi.org/10.1016/j.tust.2016.09.008>.
- Franza, A., Zheng, C., Marshall, A.M. and Jimenez, R. (2021), “Investigation of soil–pile–structure interaction induced by vertical loads and tunnelling”, *Comput. Geotech.*, **139**, 104386. <https://doi.org/10.1016/j.compgeo.2021.104386>.
- Gerheim Souza Dias, T. (2017), “Pile tunnel interaction”, Ph.D. Dissertation, Ghent University, Ghent, Belgium.
- Giardina, G., DeJong, M.J. and Mair, R.J. (2015), “Interaction between surface structures and tunnelling in sand: Centrifuge and computational modelling”, *Tunn. Undergr. Sp. Tech.*, **50**, 465-478. <https://doi.org/10.1016/j.tust.2015.07.016>.
- Hemeda, S. (2022), “Geotechnical modelling and subsurface analysis of complex underground structures using PLAXIS 3D”, *Int. J. Geo-Eng.*, **13**(9). <https://doi.org/10.1186/s40703-022-00174-7>.
- Hemeda, S. (2024), “Experimental and finite element assessment of stabilizing configurations for underground heritage sites”, *Heritage Sci.*, **12**(291). <https://doi.org/10.1186/s40494-024-01384-1>
- Jongpradist, P., Kaewsri, T., Sawatpamich, A., Suwansawat, S., Youwai, S., Kongkitkul, W. and Sunitsakul, J. (2013), “Development of tunneling influence zones for adjacent pile foundations by numerical analyses”, *Tunn. Undergr. Sp. Tech.*, **34**, 96-109. <https://doi.org/10.1016/j.tust.2012.11.005>.
- Liu, X., Suliman, L., Zhou, X., Wang, J., Linfeng, W. and Elmageed, A.A. (2022), “Settlement characteristic due to excavate parallel tunnels in a fill-rock slope: Model test and numerical analysis”, *Rock Mech. Rock Eng.*, **55**(11), 7125-7143. <https://doi.org/10.1007/s00603-022-02961-1>.
- Losacco, N., Burghignoli, A. and Callisto, L. (2014), “Uncoupled evaluation of the structural damage induced by tunnelling”, *Geotechnique*, **64**(8), 646-656. <https://doi.org/10.1680/geot.13.P.213>.
- Mahmood, K., Kim, W.B. and Yang, H.S. (2011), “A parametrical study of tunnel-pile interaction using numerical analysis”, *Geosyst. Eng.*, **14**(4), 169-174. <https://doi.org/10.1080/12269328.2011.10541347>.
- Marshall, A.M. (2012), “Tunnel-pile interaction analysis using cavity expansion methods”, *J. Geotech. Geoenviron. Eng.*, **138**(10), 1237-1246. [https://doi.org/10.1061/\(ASCE\)GT.1943-5606.0000709](https://doi.org/10.1061/(ASCE)GT.1943-5606.0000709).

- Marshall, A.M. and Haji, T. (2015), "An analytical study of tunnel–pile interaction", *Tunn. Undergr. Sp. Tech.*, **45**, 43-51. <https://doi.org/10.1016/j.tust.2014.09.001>.
- Meguid, M.A. and Mattar, J. (2009), "Investigation of tunnel-soil-pile interaction in cohesive soils", *J. Geotech. Geoenviron. Eng.*, **135**(7), 973-979. [https://doi.org/10.1061/\(ASCE\)GT.1943-5606.0000004](https://doi.org/10.1061/(ASCE)GT.1943-5606.0000004).
- Mirhabibi, A. and Soroush, A. (2013), "Effects of building three-dimensional modeling type on twin tunneling-induced ground settlement", *Tunn. Undergr. Sp. Tech.*, **38**, 224-234. <https://doi.org/10.1016/j.tust.2013.07.003>.
- Nguyen, V.M. and Nguyen, Q.P. (2015), "Analytical solution for estimating the stand-up time of the rock mass surrounding tunnel", *Tunn. Undergr. Sp. Tech.*, **47**, 10-15. <https://doi.org/10.1016/j.tust.2014.12.003>.
- Sohaie, H., Namazi, E., Hajihassani, M. and Marto, A. (2020), "A review on tunnel–pile interaction applied by physical modeling", *Geotech. Geol. Eng.*, **38**(4), 3341-3362. <https://doi.org/10.1007/s10706-020-01240-6>.
- Tsinidis, G. (2018), "Response of urban single and twin circular tunnels subjected to transversal ground seismic shaking", *Tunn. Undergr. Sp. Tech.*, **76**, 177-193. <https://doi.org/10.1016/j.tust.2018.03.016>.
- Zhang, Z., Huang, M., Xu, C., Jiang, Y. and Wang, W. (2018), "Simplified solution for tunnel-soil-pile interaction in Pasternak's foundation model", *Tunn. Undergr. Sp. Tech.*, **78**, 146-158. <https://doi.org/10.1016/j.tust.2018.04.025>.

## Abbreviations

- E*: Modulus of elasticity  
*C*: cohesion  
 $\Phi$ : friction angle  
 $\mu$ : Poisson ratio  
 $\gamma$ : unit weight  
*R*: The proposed ratio  
*D*: Tunnel diameter  
*d*: Pile diameter